Transmission System and Microgrid Co-optimization Model

Nomenclature

Indices

t a time period (time interval from the beginning through the end of a period)

g TS network generator index

Parameters

T length of the planning horizon

G total number of generators in the TS

$\overline{R}_g$ TS generator upper ramp rate limit

$\underline{R}_g$ TS generator lower ramp rate limit

$\overline{P}_g$ TS generator generation upper bound

$\underline{P}_g$ TS generator generation lower bound

$Line$ TS line limit

C_g TS generater g cost

C_g^r TS generater g reserve cost

C_g^c TS generator g commitment cost

GSF TS generation shift factor matrix

W^f forecasted wind power

W^{up} positive wind deviation from the forecast

W^{dn} negative wind deviation from the forecast

N_b number of buses in the TS

L_t TS load power vector in hour t

$\underline{L}_t^d$ MG aggregated dispatchable load lower bound in hour t

$\overline{L}_t^d$ MG aggregated dispatchable load upper bound in hour t

L_t^i MG inelastic load in time t

$\overline{B}$ MG storage energy state max level

$\underline{B}$ MG storage energy state min level

C^b MG storage energy maintenance cost

C_t^{m1} MG generation linear cost

C_t^{m2} MG generation quadratic cost

C_t^d MG utility for consuming dispatchable load in the MG in hour t

C^{dr1} MG linear demand response cost

C^{dr2} MG quadratic demand response cost

$\overline{P}^m$ MG generation upper bound

$\underline{P}^m$ MG generation lower bound

$\underline{P}^b$ MG storage discharging limit

$\overline{P}^b$ MG storage charging limit

$\overline{P}_t^d$ DR lower price cap in period t

ϵ constraint violation probability

Variables

$r_{g,t}^{up}$ TS generator g upward reserve in hour t

$r_{g,t}^{dn}$ TS generator g downward reserve in hour t

p_t^{dr} demand response price in hour t

$p_{g,t}$ TS generator g generation in hour t

b_t MG storage energy state in hour t

p_t^{ex} MG exported power in hour t

p_t^{im} MG imported power in hour t

p_t^b MG storage power output in hour t

l_t^d MG aggregated dispatchable load in hour t

dr_t^{up} MG storage power output in hour t

dr_t^{dn} MG aggregated dispatchable load in hour t

p_t^{inj} bus power injection vector in hour t

$w_{g,t}$ TS generator commitment variable in hour t for generator g

Acronyms

TS   transmission system

DL   dispatchable load

WP   wind penetration

MG   microgrid

DR   demand response

DG   distributed generation

1. Introduction

Future power systems is envisioned to move towards a sustainable and decentralized system with a high penetration of renewable energy and distributed generation [1], MGs will play a critical role in this evolution as they feature distributed local generation, energy storage, and demand response and cater the need of increased need for flexibility of the future systems. With the possibility of numerous MG connected to the TS and exchanging power with the TS, the operations of power systems will change dramatically. Each MG could be view as an independent entity with its own operation objective which could conflict with the TS's. A proper way to co-optimize the two systems will thus become very important for the efficient operation of the whole system in the future.

The co-optimization of TS and MG operation is a relatively new area. What has been done falls into two categories. One category [3, 4, 5, 6, 7, 8, 9, 10] focuses on the optimization of the MG operation with an abstract model for the TS. Specifically, this category models the TS as a node which connects to the MG and could buy or sell certain amount of energy from or to the MG at fixed prices. Non-consideration of

the TS characteristics makes such models less realistic as the nodal energy exchange and price information is based on the detailed model and can change over time. As a result, those models make the optimization of the MG less practical and are unable to reflect the MG's impact on the TS. The other category [11, 12, 13, 14, 15, 16, 17, 18] focuses on the TS details with an over-simplified model for the MG. In those work, MGs are normally modeled as distributed generations (DG) which can only sell energy. In reality, a MG model can not only sell energy, but also buy energy from the TS, store energy, and vary its load consumption (ie: providing DR). Therefore, MGs often have their own energy management systems and their operation should ideally be modeled as a separate optimization problem. Treating MGs as DGs once again fails to capture the true impact of MGs on the TS and does not provide any insights about the influence of TS over the MG's operation. In the future where there will very likely be many MGs connected to the TS, the drawbacks of the above two modeling approaches will make them inapplicable. In addition, the impact of DR on the TS can not be effectively studied with those two approaches as DR happens at the distribution level and requires a detailed model of the distribution side.

In this work, the operation of the TS and MG are optimized at the same time with a detailed model for each. A bilevel optimization approach is applied for this framework. Bilevel optimization is defined as a mathematical optimization problem in which one optimization problem (upper level problem) contains another optimization problem (lower level problem) [19]. There are two types of approaches to solve bilevel optimization problems. The first category applies classical methods including single-level reduction [20, 21], descent methods [22, 23], penalty function methods [24, 25], and trust-region methods [26, 27]. Most of the classical approaches deal with problems that are mathematically well-behaved; i.e., has convexity. Some strong assumptions such as continuous differentiability and lower semi-continuity are also quite common. Of those methods, the single level reduction method is the most widely used one when the lower level problem is convex and sufficiently regular. The single level reduction method is applied in this work. The second category applies evolutionary methods including genetic algorithms [28], particle swarm optimization [29], differential evolution [30], and metamodeling-based methods [31]. They normally require great computational efforts and do not provide performance guarantee. For a detailed review of different bilevel optimization methods, please refer to [19, 32].

In this work, the TS and the MG both are modeled in details. Bilevel optimization technique is used to co-optimize the two systems. In this optimization framework, the

factors that affect the renewable (ie: wind in this study) penetration level in the TS and the operation cost of the two systems are analyzed. Recommendations on how to improve the wind penetration level and reduce the system operation cost are given. The key contributions of this work are summarized below:

(1) Bilevel optimization framework is proposed for the co-optimization of TS and MG as well as the co-optimization of the energy market and ancillary service market.

(2) A detailed TS model with network and detailed MG model are for the first time applied in the co-optimization framework.

(3) DR is decoupled from the TS level and modeled at the distribution level, which provides a more realistic optimization model.

(4) Factors that affect the system wind penetration level and operation cost are reviewed.

The structure of the paper is as follows; the bilevel optimization model is discussed in section 3. Numerical results for are reported in Section 4. Concluding remarks and future research directions are given in Section 5.

2. Problem Description

2.1. Transmission System Problem

The TS has a network of transmission lines and buses. Traditional and renewable generation units, loads and MGs are connected to different buses in the network. The TS solves a day ahead market unit commitment problem, which is a co-optimization of the energy market and ancillary service market. For the energy market optimization, the TS tries to minimize the cost of meeting the system demand with its own generation or energy from MGs. For the ancillary service market optimization, the TS minimizes the cost of providing enough reserve to account for the renewable forecast uncertainty. The reserve service could either come from the TS generator's reserve or the MG's DR. The TS objective function minimizes the energy and ancillary service cost at the same time.

2.2. Microgrid Problem

The microgrid has an aggregated dispatchable load and an aggregated non-dispatchable load, an energy storage unit, and a distributed generation. In the day-ahead market, the MG solves an optimal dispatch problem. The dispatchable load is optimized at some point in between its upper and lower bound. The difference between the upper/lower

bound and its set point could be used to provide upward/downward DR. The objective of the MG is to minimize the cost of meeting its demand either by its distributed generation or importing power from the TS and maximize the revenue of providing DR

2.3. Co-operation Mode

The TS and MG could work in two modes. The first mode is standalone mode, in which the two systems are totally separated from each other. In this mode, the two systems could not exchange energy and the MG could not provide DR to the TS. The second mode in co-optimization mode. Under our bilevel optimization framework, the TS decides the price of MG energy import and export as well as the price for purchasing MG DR, the MG responds to those prices by exchanging a certain amount of energy with the TS and selling a certain amount of DR to the TS.

The co-optimization between the TS and MG is illustrated in Fig. 1
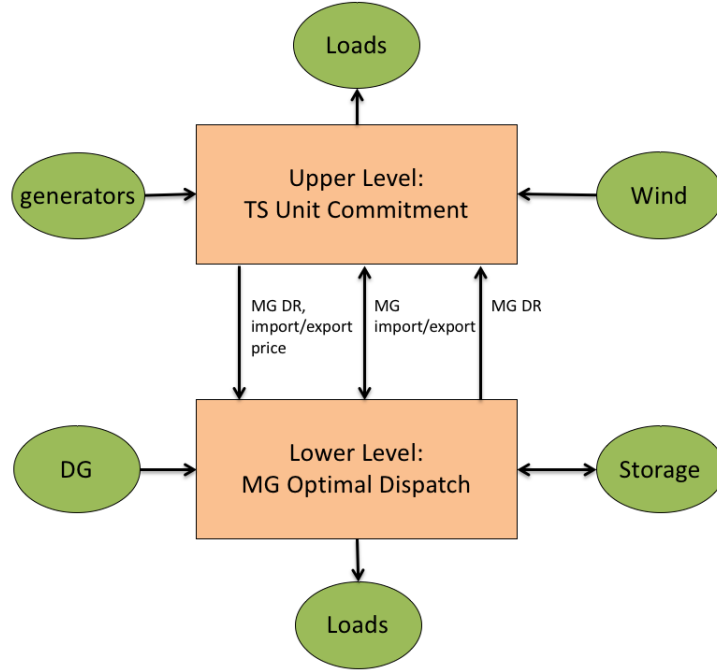
Figure 1: Co-optimization between the TS and MG

2.4. Renewable Forecast Uncertainty Management

In this work, we use a robust approach to manage the uncertainty in renewable forecast. Specifically, for a renewable generation forecast and a set of possible generation scenarios, we calculate the upward/downward forecast deviation by taking the difference of the hourly maximum/minimum generation scenario and the hourly forecast. The

downward/upward TS generation reserve and upward/downward MG DR are used to account for the upward/downward renewable forecast deviation.

3. Optimization Model

In this section, the structure of the bi-level optimization problem is described. The general formulation of a bilevel optimization is given below:

$$\min_{x \in X, y \in Y} F(x, y)$$

$$\text{st: } G_i(x, y) \leq 0, \text{for } i \in \{1, 2, ..., I\}$$

$$H_k(x, y) = 0, \text{for } k \in \{1, 2, ..., K\} \tag{1}$$

$$y \in \operatorname*{argmin}_{y \in Y}\{f(x, y) : g_j(x, y) \leq 0, \text{for } j \in \{1, 2, ..., J\},$$

$$h_m(x, y) = 0, \text{for } m \in \{1, 2, ..., M\}\}$$

In the above formulation, $x, F(x, y), (G_i, H_k)$ are the optimization variables, objective function and constraints of the upper level problem. Whereas, $y, f(x, y), (g_i, h_m)$ are the optimization variables, objective function and constraints of the lower level problem. According to this formulation, the bilevel formulation of the TS and MG co-optimization is given in the following sections.

3.1. Upper Level Problem: TS Unit Commitment Problem

The upper level transmission day-ahead unit commitment problem seeks to compute the optimal operation schedule including the generator commitment status $w_{g,t}$, generation output $p_{g,t}$, upward and downward generator's reserve $R^{up}_{g,t}$, $R^{dn}_{g,t}$, MG DR price $P^{dr}_{g,t}$, and the MG energy import and export price c^{im}_t, c^{ex}_t to minimize the total TS operation cost. The optimization variables are denoted by the vector x_t, and include:

$$x_t = [w_{g,t}, p_{g,t}, r^{up}_{g,t}, r^{dn}_{g,t}, p^{dr}_t, c^{im}_t, c^{ex}_t]$$

The objective of the upper level optimization problem is to minimize the TS operation cost including the generator commitment cost, generation cost, reserve cost, energy exchange cost with the MG and the MG DR cost.

Objective function:

$$
\begin{aligned}
F(\{x_t\}_{t=1}^T) &= \sum_{t=1}^T \sum_{g=1}^G (C^c_{g,t} w_{g,t} + C_{g,t} p_{g,t} + C^r_g (r^{up}_{g,t} + r^{dn}_{g,t}) \\
&\quad - p^{im}_t c^{im}_t + p^{ex}_t c^{ex}_t \\
&\quad + p^{dr}_t (dr^{up}_t + dr^{dn}_t))
\end{aligned}
$$

The constraints of the TS are listed below.

Power flow constraints:

$$-Line \leq GSF * pinj_t \leq Line, t \in 1, ..., T \tag{2}$$

$$-Line \leq GSF * pinj_t^* \leq Line, t \in 1, ..., T \tag{3}$$

$p_{inj,t}$ is the DC net power injection vector (ie: generation + wind - demand) for all the buses in each hour. $p_{inj,t}^*$ incorporates the wind forecast error, generator reserve and MG DR on top of $p_{inj,t}$. Eqn (2),(3) bound the transmission line flows within the flow limits.

Generator constraints:

$$\underline{P}_g \leq p_{g,t} \leq \overline{P}_g, t \in 1, ..., T \tag{4}$$

$$(p_{g,t} + r_{g,t}^{up}) - (p_{g,t-1} - r_{g,t-1}^{dn}) \leq \overline{R}_g, t \in 2, ..., T \tag{5}$$

$$\underline{R}_g \leq (p_{g,t} - r_{g,t}^{dn}) - (p_{g,t-1} + r_{g,t-1}^{up}), t \in 2, ..., T \tag{6}$$

Eqn (4) bounds the generator generation within its capacities. Eqn (5),(6) satisfy the generator ramping capability.

Power balance constraint:

$$\sum_{g=1}^{G} p_{g,t} + \mathbf{1}_{1 \times N_b} * L_t + W^f = P_t^{im} - P_t^{ex}, , t \in 1, ..., T \tag{7}$$

where $\mathbf{1}_{1 \times N_b}$ is a vector of length N_b filled with 1's. The dot product $\mathbf{1}_{1 \times N_b} * L_t$ gives the total load in the system. Eqn (7) balances the system power supply and demand.

Reserve constraints:

$$W_t^{up} \leq DR_t^{up} + \sum_{g=1}^{G} r_{g,t}^{dn}, t \in 1, ..., T \tag{8}$$

$$W_t^{dn} \leq Dr_t^{dn} + \sum_{g=1}^{G} r_{g,t}^{up}, t \in 1, ..., T \tag{9}$$

Eqn (8), (9) ensure enough generator reserve and MG DR to compensate the possible wind forecast deviation.

Finally, the TS unit commitment problem is formulated as:

$$\min_{\{x_t\}_{t=1}^{T}} F\left(\{x_t\}_{t=1}^{T}\right)$$

$$\text{s.t. } (1) - (10)$$

$$\tag{10a}$$

3.2. Lower Level Problem: MG Operation Optimization

A comprehensive MG is considered in this work. The MG consists of distributed generation (DG), a storage unit, aggregated dispatchable and non-dispatchable loads, and is able to exchange power with the main grid.

The goal of the MG optimal dispatch model is to compute the generation schedule $p_{g,t}^m$, the battery power output p_t^b, the battery charging and discharging decision p_t^b, MG energy import p_t^{im} and export p_t^{ex} schedule, dispatchable load profile l_t^d, the upward/downward DR dr_t^{up}, dr_t^{dn} provided by the dispachable load, and the storage energy state b_t. The lower level optimization variables are denoted by the vector y_t, and include:

$$y_t = [p_{g,t}^m, p_t^b, p_t^{im}, p_t^{ex}, dr_t^{up}, dr_t^{dn}, l_t^d, b_t]$$

The objective of the MG optimization is to minimize the MG operation cost including its generation cost, battery maintenance cost, energy exchange cost with the TS, and DR cost and maximize its dispatchable load utility and DR revenue.

Objective function:

$$
\begin{aligned}
f(\{y_t\}_{t=1}^T) = \sum_{t=1}^T (&C_g^{m1} p_{g,t}^m + C_g^{m2} p_{g,t}^m p_{g,t}^m + C^b b_t + p_t^{im} c_t^{im} - p_t^{ex} c_t^{ex} \\
&+ C^{dr1}(DR_{g,t}^{up} + DR_{g,t}^{dn}) + C^{dr2}(DR_{g,t}^{up} DR_{g,t}^{up} + DR_{g,t}^{dn} DR_{g,t}^{dn}) \\
&- C_t^d l_t^d - p_t^{dr}(dr_t^{up} + dr_t^{dn}))
\end{aligned}
$$

The constraints for the MG are given below. The λ and μ variables next to the constraints are the dual variables associated with the corresponding inequality and equality constraints.

Generator constraints:

$$\underline{P}^m \le p_{g,t}^m \le \overline{P}^m, \lambda_{1,t}, \lambda_{2,t}, t \in 1, ..., T \tag{11}$$

Eq (11) limits the generator's output within the upper and lower bound.

Dispatchable load constraint:

$$\underline{L}_t^d \le l_t^d \le \overline{L}_t^d, \lambda_{3,t}, \lambda_{4,t}, t \in 1, ..., T \tag{12}$$

Eq (12) constrains the dispatchable loads within predefined bounds.

DR constraints:

$$l_t^d + dr_t^{up} \leq \overline{L}_t^d, \lambda_{5,t}, t \in 1, ..., T \tag{13}$$

$$l_t^d - dr_t^{dn} \geq \underline{L}_t^d, \lambda_{6,t}, t \in 1, ..., T \tag{14}$$

$$0 \leq dr_t^{up} \leq W^{up}, \lambda_{7,t}, \lambda_{8,t}, t \in 1, ..., T \tag{15}$$

$$0 \leq dr_t^{dn} \leq W^{dn}, \lambda_{9,t}, \lambda_{10,t} t \in 1, ..., T \tag{16}$$

Eq (13), (14) limit the DR of dispatchable load within the dispatachable load bounds. Also the amount of DR could not exceed the wind forecast deviation, which is reflected in Eq (15), (16).

Storage constraints:

$$\underline{P}^b \leq p_t^b \leq \overline{P}^b, \lambda_{11,t}\lambda_{12,t}, t \in 1, ..., T \tag{17}$$

$$\underline{B} \leq b_t \leq \overline{B}, \lambda_{13,t}, \lambda_{14,t}, t \in 1, ..., T \tag{18}$$

$$b_t = B_{t-1} + p_{t-1}^b, \mu_{1,t}, t \in 1, ..., T \tag{19}$$

Eq (17) and (18) restrict the storage's output power and the energy state to their upper and lower bounds. Equation (19) shows the transition of the storage energy state from one period to the next. A positive/negative p_t^b value corresponds to charging/discharging of the battery.

Import and Export constraints:

$$0 \leq p_t^{im}, \lambda_{15,t}, t \in 1, ..., T \tag{20}$$

$$0 \leq p_t^{ex}, \lambda_{16,t}, t \in 1, ..., T \tag{21}$$

The MG import and export power is defined to be non-negative as shown in Eqn (20), (21).

Power balance constraint:

$$p_t^m - p_t^b - L_t^i - l_t^d = p_t^{ex} - p_t^{im}, \mu_{2,t}, t \in 1, ..., T \tag{22}$$

Eq (22) ensures the power balance within the MG system.

Finally, the MG optimal dispatch can be formulated as:

$$\min_{\{y_t\}_{t=1}^T} f\left(\{y_t\}_{t=1}^T\right)$$
$$\text{s.t. } (12) - (25)$$

3.3. Reformulation to a Single Level Problem

If the lower level problem is convex and satisfies certain regularity conditions [33], it can be replaced by its Karush-Kuhn-Tucker(KKT) conditions [19], the formulation in (1) becomes a single -level problem reformulation as follows:

$$\min_{x \in X, y \in Y} F(x, y)$$

st: $G_i(x, y) \leq 0, \text{for } i \in \{1, 2, ..., I\}$

$H_k(x, y) = 0, \text{for } k \in \{1, 2, ..., K\}$

$g_i(x, y) \leq 0, \text{for } j \in \{1, 2, ..., j\}$

$h_m(x, y) \leq 0, \text{for } m \in \{1, 2, ..., M\}$

dual feasibility: $\lambda_i \geq 0, \text{for } i \in \{1, 2, ..., i\}$

complementary slackness: $\lambda_i * g_i(x, y) = 0, \text{for } i \in \{1, 2, ..., i\}$

stationarity: $\nabla L(x, y, \lambda, \mu) = 0$

where :

$$L(x, y, \lambda) = f(x, y) + \sum_{i=1}^{J} \lambda_i g_i(x, y) + \sum_{m=1}^{M} \mu_m h_m(x, y)$$

The lower level problem in this study is a convex optimization problem and satisfies Slater's condition, which is one of the sufficient conditions for strong duality theorem [33]. Therefore, the lower level problem could be replaced by its KKT conditions. The KKT conditions are given below:

Stationarity:

For stationarity, the derivative of the lagrangian function $L(x, y, \lambda)$ is taken with respect to each optimization variable. For example, eq(24) is the derivative of the lagrangian function with respect to p_t^m.

$$C^m + \lambda_{2,t} - \lambda_{1,t} + \mu_{2,t} = 0, t \in 1, ..., T \tag{24}$$

$$- C^d - \lambda_{4,t} + \lambda_{3,t} - \mu_{2,t} = 0, t \in 1, ..., T \tag{25}$$

$$C^b + \lambda_{13,t} - \lambda_{14,t} + \mu_{1,t} = 0, t \in 1, ..., T \tag{26}$$

$$c_t^{im} - \lambda_{14,t} - \mu_{2,t} = 0, t \in 1, ..., T \tag{27}$$

$$- c_t^{ex} - \lambda_{15,t} + \mu_{2,t} = 0, t \in 1, ..., T \tag{28}$$

$$\lambda 8_t - \lambda_{11,t} - \mu_{1,t} - \mu_{2,t} = 0, t \in 1, ..., T \tag{29}$$

$$- P_t^{dr} - \lambda_{8,t} - \lambda_{7,t} + \lambda_{5,t} = 0, t \in 1, ..., T \tag{30}$$

$$- P_t^{dr} - \lambda_{10,t} - \lambda_{9,t} + \lambda_{6,t} = 0, t \in 1, ..., T \tag{31}$$

11

Dual feasibility:

For dual feasibility, all dual variables need to be non-negative.

$$\lambda_{1,t}...\lambda_{16,t}, t \in 1, ..., T \geq 0 \tag{32}$$

Complementary slackness:

For complementary slackness, the product of the dual variables and their corresponding inequalities need to be zero.

$$\lambda_{1,t} * (P_t^m - \underline{P}^m) = 0, t \in 1, ..., T \tag{33}$$

$$\lambda_{2,t} * (P_t^m - \overline{P}^m) = 0, t \in 1, ..., T \tag{34}$$

$$\lambda_{3,t} * (l_t^d - \overline{L}_t^d) = 0, t \in 1, ..., T \tag{35}$$

$$\lambda_{4,t} * (l_t^d - \underline{L}_t^d) = 0, t \in 1, ..., T \tag{36}$$

$$\lambda_{5,t} * (dr_t^{up} + l_t^d - \overline{l}_t^d) = 0, t \in 1, ..., T \tag{37}$$

$$\lambda_{6,t} * (-dr_t^{dn} - l_t^d + \underline{l}_t^d) = 0, t \in 1, ..., T \tag{38}$$

$$\lambda_{7,t} * (dr_t^{up}) = 0, t \in 1, ..., T \tag{39}$$

$$\lambda_{8,t} * (dr_t^{up} - W^{up}) = 0, t \in 1, ..., T \tag{40}$$

$$\lambda_{9,t} * (dr_t^{dn}) = 0, t \in 1, ..., T \tag{41}$$

$$\lambda_{10,t} * (dr_t^{dn} - W^{dn}) = 0, t \in 1, ..., T \tag{42}$$

$$\lambda_{11,t} * (p_t^b - \overline{p}_t^b) = 0, t \in 1, ..., T \tag{43}$$

$$\lambda_{12,t} * (p_t^b - \underline{p}_t^b) = 0, t \in 1, ..., T \tag{44}$$

$$\lambda_{13,t} * (b_t - \overline{B}) = 0, t \in 1, ..., T \tag{45}$$

$$\lambda_{14,t} * (b_t - \underline{B}) = 0, t \in 1, ..., T \tag{46}$$

$$\lambda_{15,t} * (b_t) = 0, t \in 1, ..., T \tag{47}$$

$$\lambda_{16,t} * (b_t) = 0, t \in 1, ..., T \tag{48}$$

This reformulation is not easy to solve mainly due to the non-convexity in the complementary slackness and bilinear terms in the objective function. The big-M reformulation is used to transform the complementary conditions to mixed integer constraints. The technical details of the Big-M method is given in the appendix.

According to strong duality theorem, the optimal objective function value of the lower level optimization dual problem equals the optimal objective function value of the lower level optimization primal problem. As a result, the bilinear terms $-p_t^{im}c_t^{im} + p_t^{ex}c_t^{ex} + p_t^{dr}(dr_t^{up} + dr_t^{dn})$ in the lower level objective function, which also appear in the upper level objective function, could be expressed as linear terms using the objective

function of the dual problem. The lower level dual problem objective function is as follow:

$$
\begin{aligned}
D(\{\lambda_t, \mu_t\}_{t=1}^T) &= \sum_{t=1}^T (-C^{dr2} dr_t^{dn} dr_t^{dn} - C^{dr2} dr_t^{up} dr_t^{up} - C_g^{m2} p_{g,t}^m p_{g,t}^m \\
&- \mu_{2,t} L_t^i + \lambda 1_t \underline{P}^m - \lambda_{2,t} \overline{P}^m - \lambda_{3,t} underline L_t^d + \lambda_{4,t} \overline{L}_t^d - \lambda_{5,t} \underline{L}_t^d + \lambda_{6,t} \overline{L}_t^d \\
&- \lambda_{8,t} \overline{W}^{up} + \lambda_{10,t} \overline{W}^{dn} - \lambda_{11,t} \overline{P}_t^b + \lambda_{12,t} \underline{P}_{-t}^b - \lambda_{13,t} \overline{B} + \lambda_{14,t} \underline{B})
\end{aligned}
$$

The bilinear terms $-p_t^{im} c_t^{im} + p_t^{ex} c_t^{ex} + p_t^{dr} (dr_t^{up} + dr_t^{dn}$ in the upper level objective function are represented as:

$$
\sum_{t=1}^T (C_g^{m1} p_{g,t}^m + C_g^{m2} p_{g,t}^m p_{g,t}^m + C^b b_t + C^{dr1} dr_{g,t}^{up} + dr_{g,t}^{dn} +
$$

$$
+ C^{dr2} (dr_{g,t}^{up} dr_{g,t}^{up} + dr_{g,t}^{dn} dr_{g,t}^{dn}) - C_t^d l_t^d) - D(\{\lambda_t, \mu_t\}_{t=1}^T)
$$

The reformulated upper level objective function is as follow:

$$
\begin{aligned}
F\left(\{x_t, y_t, \lambda_t, \mu_t\}_{t=1}^T\right) &= \sum_{t=1}^T \sum_{g=1}^G (C_{g,t}^c w_{g,t} + C_{g,t} p_{g,t} + C_g^r (r_{g,t}^{up} + r_{g,t}^{dn}) \\
&+ C_g^{m1} p_{g,t}^m + C_g^{m2} p_{g,t}^m p_{g,t}^m + C^b b_t + C^{dr1} dr_{g,t}^{up} + dr_{g,t}^{dn} \\
&+ C^{dr2} (dr_{g,t}^{up} dr_{g,t}^{up} + dr_{g,t}^{dn} dr_{g,t}^{dn}) - C_t^d l_t^d) - D(\{\lambda_t, \mu_t\}_{t=1}^T)
\end{aligned}
$$

The reformulated single level problem has the following format:

$$
\min_{\{x_t, y_t, \lambda_t, \mu_t\}_{t=1}^T} F\left(\{x_t, y_t, \lambda_t, \mu_t\}_{t=1}^T\right)
$$

$$
st: (1) - (50)
$$

With the big-M reformulation, a set of binary variables and additional constants are introduced. The bilevel problem becomes a single level mixed integer linear problem and could thus be solved with a wide range of commercial solvers such as Cplex and Gurobi.

4. Numerical Results

In this section, the transmission model described in Section 3 is applied to the IEEE 30-bus system, shown in Fig. 2. Interested readers are referred to [34] for detailed parameters of the TS. The MG export cost c_t^{ex} is defined to be $0.9 * c_t^{im}$. The parameters of the 25 MW MG is listed in the appendix. Multiple wind farms are positioned at different buses in the TS to provide renewable generation. A comprehensive MG is considered in this work. The MG consists of a generator, a storage unit, DL and non-DL, and is able to operate in islanded mode and grid-connected mode. The parameter values of the 25 MW MG are listed in the appendix.
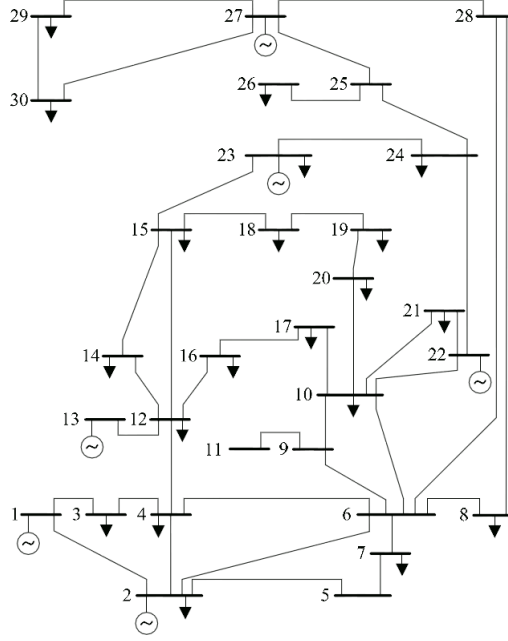
Figure 2: IEEE 30 Bus System

The wind data for the wind farms in the TS are selected from the NREL-Eastern Wind Integration Study dataset [35]. Using three years of data, 24-hour trajectories are grouped to identify a set of 54 similar trajectories, with a common initial condition. The set of trajectories was used to represent the realizations of a similar forecast. The central trajectory of the group was selected as the wind forecast, and the remaining were used to estimate the distribution of forecast errors, as described in [36]. From the forecast error distribution, 10000 scenarios are used to generate a robust wind error scenario set.

The objective of this work is to analyze different factors that affect the WP in the TS and the operational cost of the two systems in this co-optimization framework as well as the standalone framework. To this end, this section is divided into a WP result part and system cost part.

4.1. WP Results

The definition of WP is based on the wind power capacity penetration defined by the European Wind Energy Association [37]. It is the ratio of the installed wind capacity divided by the peak system load.

4.1.1. Location of Wind in the System

To generate some benchmarks, a wind farm is positioned at different buses in the TS with no MG. The maximum WP in each case is recorded. The results for some

14

representative bus are given in Table1.

Wind Bus	Max WP	Reason
5	38%	Use up generator reserve
8	28%	Reach transmission limit
15	38%	Use up generator reserve
30	28%	Reach transmission limit
8 and 30	38%	Use up generator reserve

Table 1: WP at different buses

As the TS has a network with limits on transmission lines, different buses have different capacities in terms of renewable injection. Table 1 shows that bus 8 and 30 allows smaller WPs compared to bus 5 and 15 as bus 8 and 30 are connected to transmission lines with smaller capacity. For bus 5 and 15, the connected line capacity is large enough to use up the generator reserve to achieve maximum WP. When there are two wind farms at bus 8 and 30, all the generator reserve is used to account for the wind forecast deviation as the combined line capacity at those two buses is large enough to use up the generator reserve. Therefore, wind farms should avoid buses with tight transmission constraints in terms of their placement. The method to find buses that are more prone to violate transmission constraints in given in [2]. As a result, wind farms should be placed at buses with generous transmission capacity and possibly at multiple locations to achieve high level of WP.

4.1.2. WP with a MG

To illustrate the effects of MG on the WP, a 25MW MG with 50% DL is connected to the wind buses in the previous section. Here the DL percentage is defined as the ratio of the maximum DL and the sum of maximum DL and non-DL. The size of the MG (25MW in this case) is defined as the generation capacity of the MG. The WP with and without the MG is given in Fig.3.
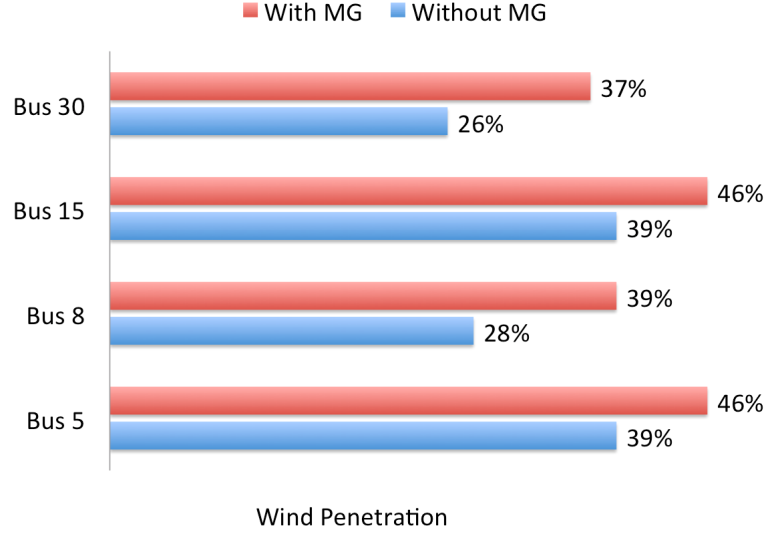
Figure 3: WP with and without MG at different buses

Fig.3 illustrates that the WP in general increases since the DR provided by the MG could act as reserve and locally offset some wind forecast error at the wind bus. The penetration increase for bus 8 and 30 is more than that of bus 5 and 15 as the MG and TS energy exchange at bus 8 and 30 frees some line capacity for the generator reserves. This case shows that the MG could alleviate congestion under the current energy exchange pricing scheme. This observation is consistent with the results in [2]. Therefore, for congestion management purpose, MGs should be placed at buses with congestions under this optimization framework. Table 2 shows the the maximum WP when the MG is placed at different buses from the wind farm bus. This table shows that when the MG and wind farm are at different buses, the WP level could only be less than that when they are at the same bus as the later case could bypass transmission constraints and directly offset wind forecast error, which is not possible for the former case.

Wind Bus	MG Bus	Max WP
5	8	45%
5	15	45%
5	30	45%
8	5	28%
8	15	28%
8	30	28%

Table 2: WP with the wind farm and MG at different buses

4.1.3. WP for different MG sizes and DL levels

As the amount of reserve is proportional to the size of the MG and the amount of DL in the MG, the WP with regards to those two factors are analyzed here. To simulate a MG with varying sizes, the MG parameters except for the ones related to the costs are scaled by the same constant. The wind farm and MG are both located at bus 5 to guarantee enough line capacity and no interference from line constraints. Fig. 4 shows WPs for different sizes of a MG with 50% of the loads being dispachable. Fig. 5 shows WPs for a 25MW MG with different levels of DLs. It can be seen from the two figures that WPs are linearly proportional to MG size and DL levels as there is more MG DR to offset the wind forecast error.
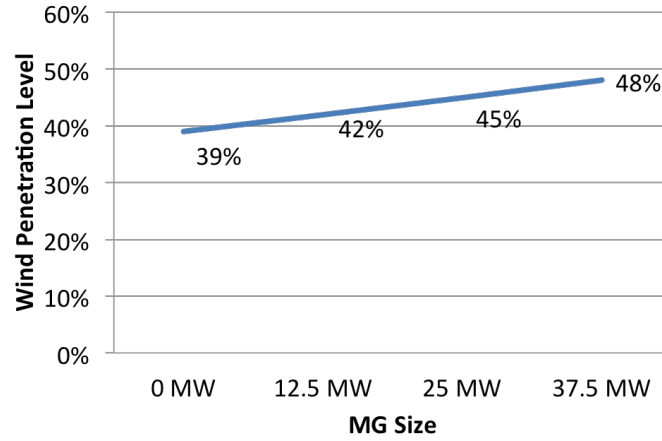
Figure 4: WP for different MG sizes

17
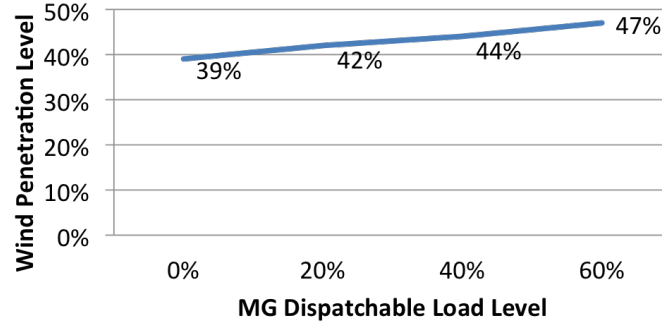
Figure 5: WP for different DL levels

4.2. System Cost Results

One goal of the TS and MG co-optimization is to reduce the individual system's operation cost. Different factors that affect the cost of the two systems are explored in this section. For the figures in this subsection, SA stands for standalone mode, while COOP stands for co-optimization mode. In the COOP mode, the MG is able to provide DR as reserve to account for the wind forecast error in the TS and exchange energy with the TS. In the SA mode, the MG is separated from the TS and thus could not exchange energy with the TS or provide any DR.

4.2.1. WP on transmission and MG cost

As WP is a key concern of the future grid and also a focus of this study, the WP is varied to see the impact on the TS and MG cost. The wind farm and a 25MW MG with 50% DL is connected to bus 5. The results are displayed in Fig. 6.
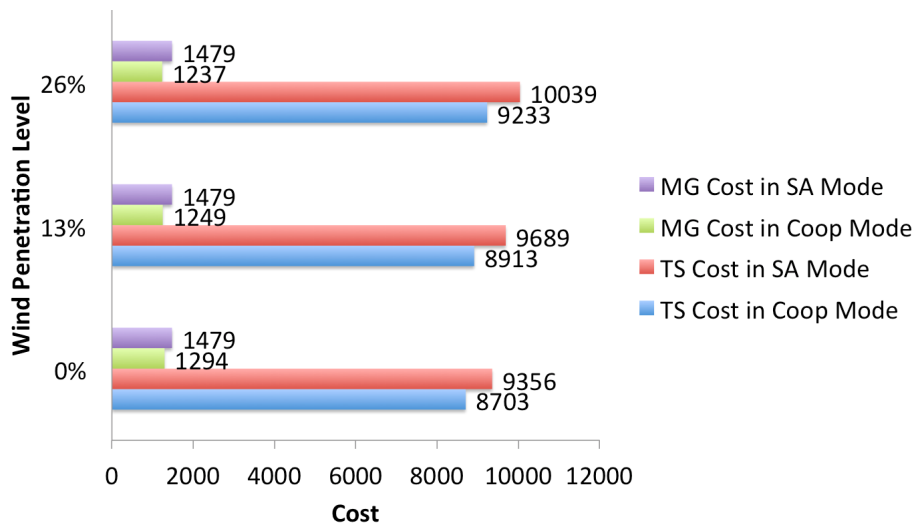
Figure 6: TS cost for different WP levels

18
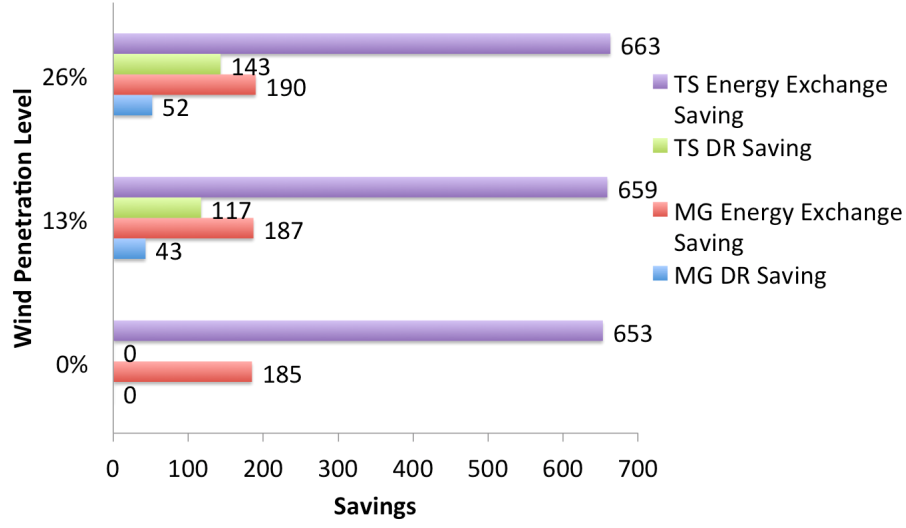
Figure 7: TS and MG savings breakdown for different WP levels

From Fig. 6, the operational costs of the two systems are smaller in the Coop mode due to the mutual benefits from the energy exchange and DR. In the SA mode, the MG cost is the same for all three cases as the MG configuration stays the same for all of them. Fig. 6 shows the break down of the MG and TS savings in terms of DR and energy exchange. When there is no wind, the difference in the operational cost between the operational modes is totally from the energy exchange benefits. As wind penetration increases, the DR savings for the MG and TS increase as more cheaper MG DR is engaged in the ancillary market. The energy exchange saving for the two systems are more or less the same for the three cases as the energy exchange price and quantity (mainly MG import) do not change much. This case study shows that the total saving in the Coop mode with a higher WP is greater for both systems.

4.2.2. MG size on transmission cost

The TS is optimized with different sizes of MG connected to bus 5 and the operation cost is reported in Fig. 8. For all the cases, the DL level in the MG is 50%. The wind farm is connected to bus 8, and a fixed 10% WP is used.
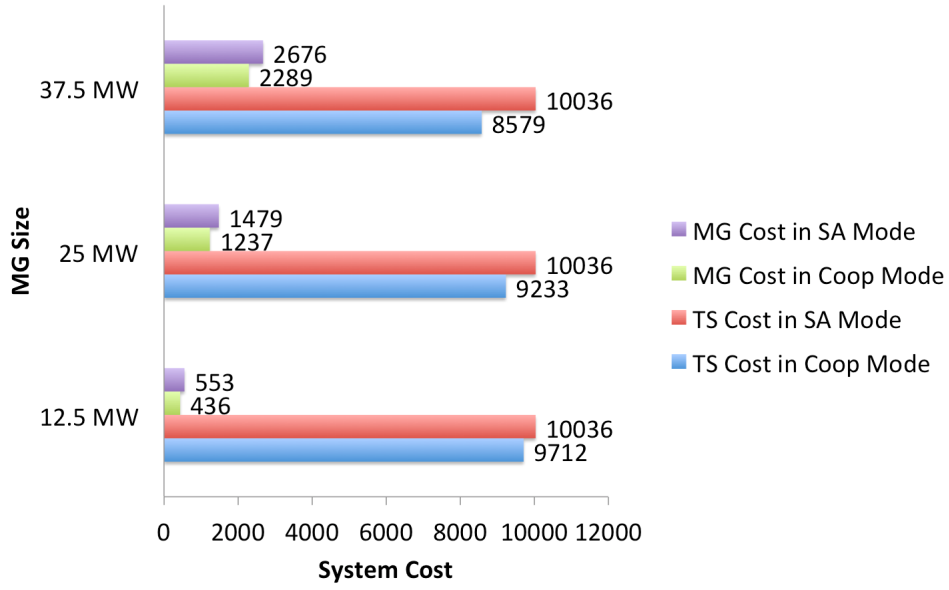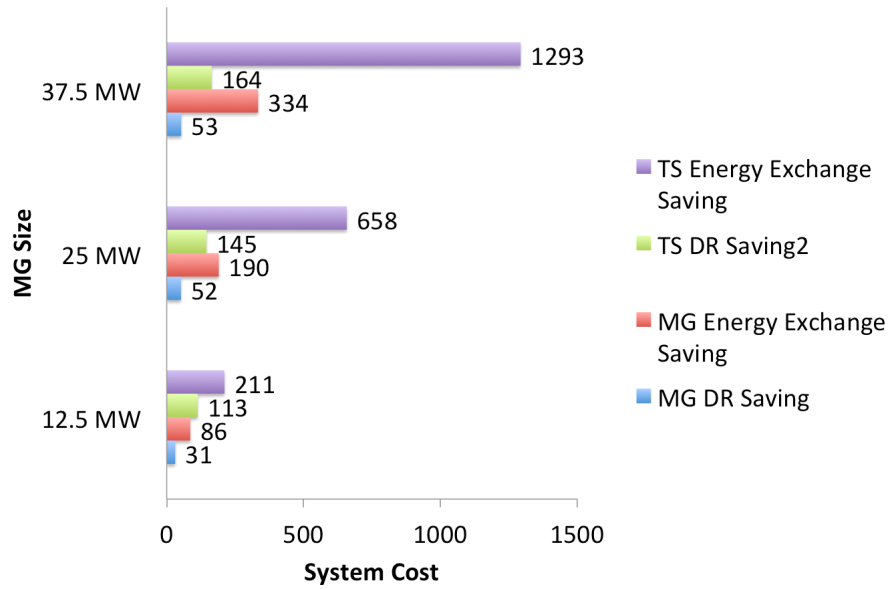
Figure 8: TS cost for different MG sizes

Figure 9: TS and MG savings breakdown for different MG sizes

From Fig. 8, it can be seen that in the Co-op mode the cost of the TS decreases with the increase in MG size. That is due to the increased volume of the DR and energy exchange with a larger MG. In addition, the individual system's cost is always smaller in the co-optimization mode compared to the standalone mode as both systems have opportunities to arbitrage in the energy exchange transactions in addition to the benefits from the reserve provision. In the SA mode, the TS cost is the same for all three cases as

the TS configuration stays the same for all of them. Fig. 9 shows the break down of the MG and TS savings in terms of DR and energy exchange. As the MG size increases, the benefits from the energy exchange for both systems increase since the energy exchange volume increases with a larger MG. The DR benefits for both systems also increase as a larger MG could provide more DR service. However the MG DR benefit does not increase much from a 25MW to a 37.5MW MG. That is because the DR price in the latter case is actually lower although the DR provision is greater. This case study shows that the total saving in the Coop mode with a bigger MG is greater for both systems.

4.2.3. MG DL level on transmission and MG cost

For the setting of a 25MW MG and 10% WP at bus 5 in the TS, the TS and MG operation cost at different levels of MG DL are reported in Fig. 10.
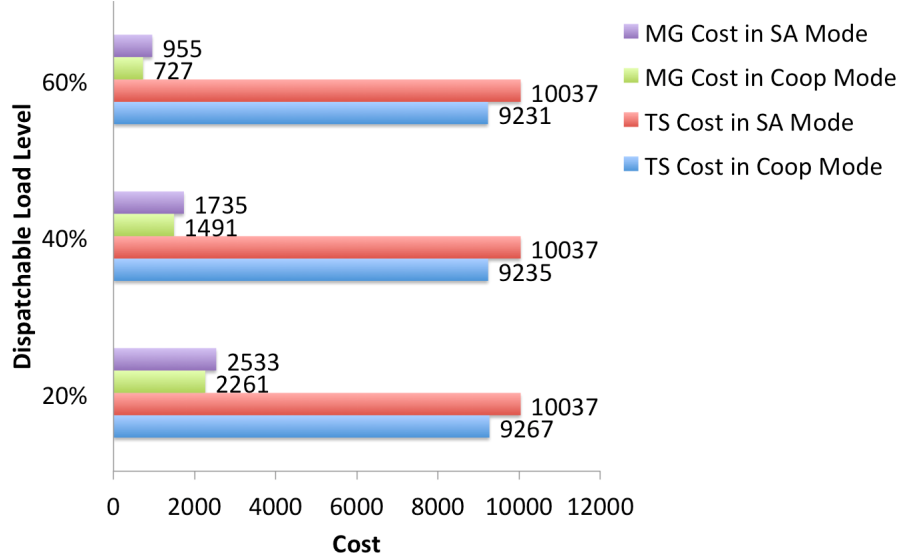

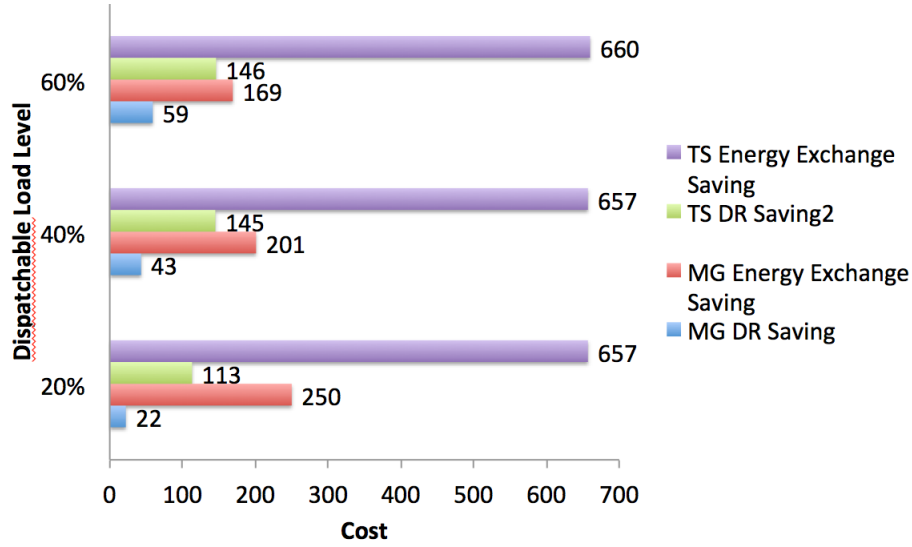Figure 10: TS cost for different MG DL levels

Figure 11: TS and MG savings breakdown for different MG DL levels

It is shown in Fig.10 that the TS cost decreases with an increasing DL level as more wind forecast error is accounted by the cheaper MG DR. However that decrease is not significant. In contrast, the MG cost decreases significantly with the increasing DL level as the MG has more DR to sell and more load flexibility. Once again, the Coop framework enables mutual financial benefits from the reserve service and energy exchange and thus reduces the cost of the two systems. The savings breakdown in Fig.11 gives further insights about the co-optimization. The energy exchange saving of the TS stays more or less the same for different dispatchable load levels as the net energy exchange quantity with the TS is more or less the same among the three cases. On the contrary, the energy exchange savings for the MG decreases with an increasing dispatchable load level. That is because the cost increasing rate of the MG in the SA mode is great than that in the Coop mode with a decreasing dispatchable load level as the Coop mode enables cost saving from energy exchange. The DR savings for both systems increase with an increasing dispatchable load level as a higher level enables more DR service. However, the DR saving for the TS from 40% to 60% DL does not increase much as the marginal cost benefit for that additional DR is very small.

4.2.4. Wind farm and MG locations on transmission and MG cost

With 10% WP, a 25MW MG with 50% DL system configuration, the location of the wind farm and the MG does not make a difference in terms of the system operation cost as this WP does not cause congestion anywhere in the system. However it is possible that a higher WP at certain buses could cause congestion and significantly increases

the system operating cost, which is a well-known fact in the power systems. The way to wisely position the MG to deal with the congestion and reduce the system cost is discussed in [2].

5. Concluding Remarks

This paper presents an analysis of a grid-connected microgrid with DR and distributed generation.

Acknowledgements

6. Appendix

6.1. Big-M Method

The complementary conditions are set of constraints with the following format:

$$\lambda_i * g_i(x, y) = 0$$

Specifically, given a sufficiently large positive value M_i and binary value ϕ_i, the complementary conditions could be reformulated as below:

$$-(1 - \phi_i) * M_i \leq g_i(x, y)$$
$$\lambda_i \leq \phi_i * M_i$$

For a detailed treatment of the Big-M method, please refer to [38].

6.2. Microgrid Parameters

The parameter values for a 25 MW MG are listed in the table below.

Parameters	Values
$\underline{L}_t^d$	6.6MW
$\overline{L}_t^d$	12MW
L_t^i	12MW
$\overline{B}$	10MW
$\underline{B}$	0MW
C^b	\$0.1/MW
C_t^{m1}	\$4/MW
C_t^{m2}	\$0.07/MW
C_t^{dr1}	\$0.4/MW
C_t^{dr2}	\$0.3/MW
C_t^d	\$6/MW
$\overline{P}_t^d$	\$1/MW
$\overline{P}^m$	25MW
$\underline{P}^m$	0MW
$\underline{P}^b$	-5MW
$\overline{P}^b$	5MW

Table 3: MG parameter values

7. References

[1] L. Anderson, L. Zéphyr, and J. Cardell, "A vision for co-optimized t&d system interaction with renewables and demand response," in *Proceedings of the 50th Hawaii International Conference on System Sciences*, 2017.

[2] J. Liu, G. Martinez, and C. L. Anderson, "Quantifying the impact of microgrid location and behavior on transmission network congestion," in *Proceedings of the 2016 Winter Simulation Conference.* IEEE Press, 2016, pp. 1745–1756.

[3] G. Carpinelli, F. Mottola, and D. Proto, "Optimal scheduling of a microgrid with demand response resources," *IET Generation, Transmission Distribution*, vol. 8, no. 12, pp. 1891–1899, 2014.

[4] S. Choi, S. Park, D. J. Kang, S. j. Han, and H. M. Kim, "A microgrid energy management system for inducing optimal demand response," *Smart Grid Communications (SmartGridComm), 2011 IEEE International Conference on*, 2011.

[5] D. Wang, S. Ge, H. Jia, C. Wang, Y. Zhou, N. Lu, and X. Kong, "A demand response and battery storage coordination algorithm for providing microgrid tie-line smoothing services," *IEEE Transactions on Sustainable Energy*, vol. 5, no. 2, pp. 476–486, April 2014.

[6] Y. Zhang, R. Wang, T. Zhang, Y. Liu, and B. Guo, "Model predictive control-based operation management for a residential microgrid with considering forecast uncertainties and demand response strategies," *IET Generation, Transmission Distribution*, vol. 10, no. 10, pp. 2367–2378, 2016.

[7] M. Ahmadi, J. M. Rosenberger, W. J. Lee, and A. Kulvanitchaiyanunt, "Optimizing load control in a collaborative residential microgrid environment," *IEEE Transactions on Smart Grid*, vol. 6, no. 3, pp. 1196–1207, May 2015.

[8] E. Mojica-Nava, C. Barreto, and N. Quijano, "Population games methods for distributed control of microgrids," *IEEE Transactions on Smart Grid*, vol. 6, no. 6, pp. 2586–2595, Nov 2015.

[9] D. T. Nguyen and L. B. Le, "Risk-constrained profit maximization for microgrid aggregators with demand response," *IEEE Transactions on Smart Grid*, vol. 6, no. 1, pp. 135–146, Jan 2015.

[10] H. P. Khomami and M. H. Javidi, "Energy management of smart microgrid in presence of renewable energy sources based on real-time pricing," in *2014 Smart Grid Conference (SGC)*, Dec 2014, pp. 1–6.

[11] M. Afkousi-Paqaleh, A. Abbaspour-Tehrani-fard, M. Rashidinejad, and K. Y. Lee, "Optimal placement and sizing of distributed resources for congestion management considering cost/benefit analysis," *Power and Energy Society General Meeting*, 2010.

[12] J. Liu, M. M. A. Salama, and R. R. Mansour, "Identify the impact of distributed resources on congestion management," *Institute of Electrical and Electronics Engineers Transactions On Power Delivery*, vol. 20, no. 3, pp. 1998–2005, 2005.

[13] S. M. H. Nabavi, S. Hajforoosh, and M. A. S. Masoum, "Placement and sizing of distributed generation units for congestion management and improvement of voltage

profile using particle swarm optimization," in *Innovative Smart Grid Technologies Asia (ISGT), 2011.* Institute of Electrical and Electronics Engineers, 2011, pp. 1–6.

[14] H. Labrini, A. Gad, R. A. ElShatshat, and M. M. A. Salama, "Dynamic graph based dg allocation for congestion mitigation in radial distribution networks," in *Power Energy Society General Meeting.* Institute of Electrical and Electronics Engineers, 2015, pp. 1–5.

[15] N. Kumar, P. Dutta, and L. Xie, "Optimal dg placement for congestion mitigation and social welfare maximization," in *North American Power Symposium (NAPS), 2011*, 2011, pp. 1–5.

[16] M. Afkousi-Paqaleh, A. R. Noory, A. A. T. F., and M. Rashidinejad, "Transmission congestion management using distributed generation considering load uncertainty," *Power and Energy Engineering Conference (APPEEC)*, pp. 1–4, 2010.

[17] C. Nayanatara, J. Baskaran, and D. P. Kothari, "Simulated annealing approach for congestion minimization using distributed power generation," *Computation of Power, Energy Information and Commuincation (ICCPEIC)*, pp. 276–281, 2015.

[18] L. Chun-Hao and A. Nirwan, "Alleviating solar energy congestion in the distribution grid via smart metering communications," *Institute of Electrical and Electronics Engineers Transactions on Parallel and Distributed Systems*, 2012.

[19] A. Sinha, P. Malo, and K. Deb, "A review on bilevel optimization: from classical to evolutionary approaches and applications," *IEEE Transactions on Evolutionary Computation*, 2017.

[20] W. F. Bialas and M. H. Karwan, "Two-level linear programming," *Management science*, vol. 30, no. 8, pp. 1004–1020, 1984.

[21] J. F. Bard and J. E. Falk, "An explicit solution to the multi-level programming problem," *Computers & Operations Research*, vol. 9, no. 1, pp. 77–100, 1982.

[22] C. D. Kolstad and L. S. Lasdon, "Derivative evaluation and computational experience with large bilevel mathematical programs," *Journal of optimization theory and applications*, vol. 65, no. 3, pp. 485–499, 1990.

[23] G. Savard and J. Gauvin, "The steepest descent direction for the nonlinear bilevel programming problem," *Operations Research Letters*, vol. 15, no. 5, pp. 265–272, 1994.

[24] Y. Lv, T. Hu, G. Wang, and Z. Wan, "A penalty function method based on kuhn–tucker condition for solving linear bilevel programming," *Applied Mathematics and Computation*, vol. 188, no. 1, pp. 808–813, 2007.

[25] D. J. White and G. Anandalingam, "A penalty function approach for solving bilevel linear programs," *Journal of Global Optimization*, vol. 3, no. 4, pp. 397–419, 1993.

[26] B. Colson, P. Marcotte, and G. Savard, "A trust-region method for nonlinear bilevel programming: algorithm and computational experience," *Computational Optimization and Applications*, vol. 30, no. 3, pp. 211–227, 2005.

[27] P. Marcotte, G. Savard, and D. Zhu, "A trust region algorithm for nonlinear bilevel programming," *Operations research letters*, vol. 29, no. 4, pp. 171–179, 2001.

[28] R. Mathieu, L. Pittard, and G. Anandalingam, "Genetic algorithm based approach to bi-level linear programming," *RAIRO-Operations Research*, vol. 28, no. 1, pp. 1–21, 1994.

[29] X. Li, P. Tian, and X. Min, "A hierarchical particle swarm optimization for solving bilevel programming problems," in *International Conference on Artificial Intelligence and Soft Computing*. Springer, 2006, pp. 1169–1178.

[30] X. Zhu, Q. Yu, and X. Wang, "A hybrid differential evolution algorithm for solving nonlinear bilevel programming with linear constraints," in *Cognitive Informatics, 2006. ICCI 2006. 5th IEEE International Conference on*, vol. 1. IEEE, 2006, pp. 126–131.

[31] G. G. Wang and S. Shan, "Review of metamodeling techniques in support of engineering design optimization," *Journal of Mechanical design*, vol. 129, no. 4, pp. 370–380, 2007.

[32] B. Colson, P. Marcotte, and G. Savard, "An overview of bilevel optimization," *Annals of operations research*, vol. 153, no. 1, pp. 235–256, 2007.

[33] J. Borwein and A. S. Lewis, *Convex analysis and nonlinear optimization: theory and examples*. Springer Science & Business Media, 2010.

[34] R. D. Zimmerman, C. E. Murillo-Sánchez, and R. J. Thomas, "Matpower's extensible optimal power flow architecture," in *Power & Energy Society General Meeting, 2009. PES'09. IEEE*. IEEE, 2009, pp. 1–7.

[35] G. L. R. W. Energy, "Eastern wind integration and transmission study," *Technical Report, National Renewable Energy Laboratory (NREL)*, 2010.

[36] C. Anderson and R. Zimmerman, "Wind output forecasts and scenario analysis for stochastic multiperiod optimal power flow," *PSERC Webinar*, pp. 1–38, 2011.

[37] E. W. E. Association *et al.*, *Wind energy-the facts: a guide to the technology, economics and future of wind power*. Routledge, 2012.

[38] W. L. Winston, M. Venkataramanan, and J. B. Goldberg, *Introduction to mathematical programming*. Thomson/Brooks/Cole Duxbury; Pacific Grove, CA, 2003, vol. 1.